Published by IOP Publishing for Sissa Medialab

Received: *February 14, 2025*
Accepted: *April 1, 2025*
Published: *May 6, 2025*

6th International Workshop on New Photon-Detector
Harbour Centre, Vancouver (BC) Canada
19–21 November 2024

Time-of-flight measurement with the ALPHA-g Barrel Scintillator detector for gravitational studies of anti-matter

G. Smith

Department of Physics and Astronomy, University of British Columbia, 6224 Agricultural Road, Vancouver, Canada
TRIUMF, 4004 Wesbrook Mall, Vancouver, Canada

E-mail: gsmith@triumf.ca

Abstract: The ALPHA-g experiment recently made headlines for the first direct measurement of the gravitational free-fall of anti-hydrogen. Crucial to this milestone is a detector system capable of accurately recording the vertical position of annihilating anti-atoms, with two critical requirements: precise localization of anti-hydrogen annihilations into the "up" or "down" regions, and effective discrimination against the cosmic ray background. To accomplish this, charged pions produced in the annihilation are tracked using a radial time projection chamber detector, and fitted to a common vertex. These pions are also detected by the "Barrel Scintillator" detector, composed of 2.6-meter plastic scintillator bars with silicon photomultipliers at both ends. The arrival time of photons at the silicon photomultipliers is used to determine the time of the pion hitting the bar. This timing information is then used as part of a multivariate analysis to reject externally incident cosmic rays. This poster showcases the time calibration procedure used to obtain time-of-flight measurement of cosmic rays in the Barrel Scintillator, and the background rejection algorithm that will be used for forthcoming ALPHA-g measurements of the gravitational behaviour of anti-hydrogen.

Keywords: Particle identification methods; Timing detectors

https://doi.org/10.1088/1748-0221/20/05/C05007

2025 JINST 20 C05007

Contents

1 Introduction to ALPHA and ALPHA-g

ALPHA is an international collaboration based at the Antiproton Decelerator (AD) at CERN. The collaboration aims to verify the fundamental symmetries between matter and anti-matter through experiments on anti-hydrogen atoms. Since trapping the first anti-hydrogen atoms in 2010 [1], ALPHA has measured a number of its spectroscopic transitions [2–5], and developed techniques such as anti-hydrogen laser cooling [6].

Recently, ALPHA has moved towards verifying a predicted symmetry of anti-matter: the equivalence of the Earth's gravitational pull on hydrogen and anti-hydrogen, which is guaranteed by the weak equivalence principle (WEP). This has necessitated the development of a new apparatus called ALPHA-g. The first measurements of anti-hydrogen taken with this apparatus were published in 2023 [7] and show no disagreement from WEP predictions.

Anti-hydrogen trapping in ALPHA-g begins with capturing around 500 000 anti-protons from CERN's ELENA decelerator ring [8] in a Penning-Malmberg charged particle trap. This anti-proton plasma is cooled via sympathetic cooling with electrons and transferred to a second Penning-Malmberg trap in ALPHA-g. Concurrently, a Na-22 radioactive source with a Surko buffer gas trap [9] is used to create a plasma of positrons. These are cooled via sympathetic cooling with laser-cooled beryllium ions, and transferred to the ALPHA-g Penning-Malmberg trap. An overview of the full apparatus is shown in figure 1.

The anti-proton and positron plasmas are combined by slowly lowering their respective trapping potentials, allowing the plasmas to combine and form anti-hydrogen. The anti-atoms with the lowest kinetic energy are trapped by a superimposed magnetic minimum trap acting on the anti-hydrogen magnetic dipole, formed by a set of octupole magnets and two solenoid mirror coils. The gravity experiment is then performed by slowly ramping down the magnetic coils responsible for vertical confinement. Atoms can escape into either an "up" region or a "down" region; the influence of gravity leads more anti-atoms to the down region. In some trials, an additional magnetic bias was applied to oppose or enhance the effect of gravity. By comparing the up/down ratio of escaped atoms to simulation, the value of g for anti-hydrogen was constrained to 0.75 ± 0.13 (stat) ± 0.16 (sim).

2025 JINST 20 C05007

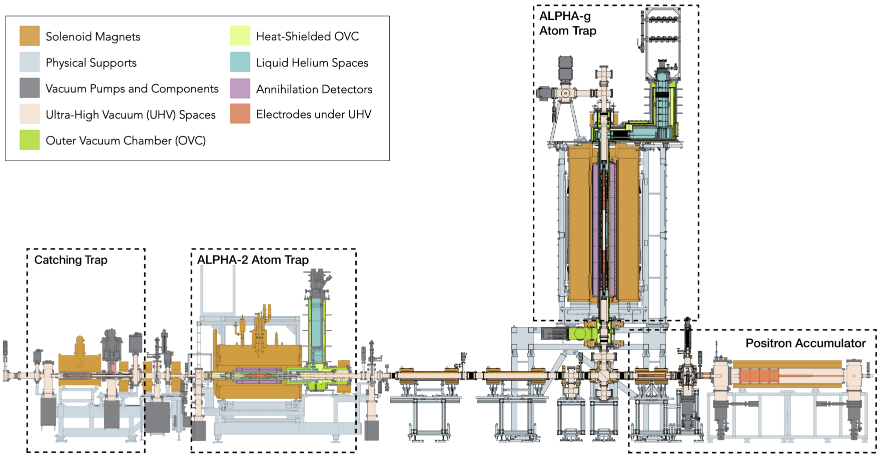

Figure 1. Overview of the ALPHA apparatus. Boxed are the catching trap, the ALPHA-2 trap (used for other studies), the positron accumulator, and the ALPHA-g trap.

2 The ALPHA-g annihilation detectors

Two detectors were built at TRIUMF to detect the annihilations of anti-hydrogen atoms and localize them to the up and down regions. The main detector is the ALPHA-g radial time projection chamber (TPC) which uses an argon-CO_2 gas mix with a drift region created by a radial electric field. Annihilating anti-atoms produce charged pions which leave a trail of ionized argon atoms along their trajectories. The freed electrons drift to the anode wires and create an electron avalanche. This induces a signal on the anode wires and on segmented cathode pads, which are combined to reconstruct the pion track in three dimensions. The set of pion tracks is then used to reconstruct the annihilation position with a vertical resolution of less than 2 cm. This process is shown in figure 2.

The TPC is sensitive to a cosmic ray rate of 70 Hz. A second detector was designed to distinguish these background events from annihilations. This barrel scintillator (BSC) detector is composed of 64 bars of EJ-200 plastic scintillator [10] of length 2.6 m and width 20 mm. The bars have a trapezoidal cross-sectional shape which allows them to fit together seamlessly surrounding the TPC. Scintillation light produced in the bars by charged particles reflects internally until reaching the ends of the bars. Each bar end is instrumented with six 6 mm square Onsemi/Sens-L MicroFJ-6005 silicon photomultipliers [11], which are coupled to the scintillator using RTV rubber.

Plastic scintillator and silicon photomultipliers (SiPMs) form a relatively fast detector, capable of measuring the time of flight of a charged particle across the BSC. The difference between the photon arrival time at the top and bottom of a bar is used to determine the position of the hit along the bar. The mean of the top and bottom photon arrival time gives the time that the charged particle crossed the bar. The difference between the hit time of different bars can be used to distinguish externally incident cosmic rays from annihilation events.

3 Barrel Scintillator time calibration

The signals from the six SiPMs at the end of a bar are combined through an analog sum. The combined signal is then split into two branches, with one branch passing through a pulse shaper, and the other digitized by a fixed-threshold comparator. The analog and digital signals are carried from the detector

2025 JINST 20 C05007

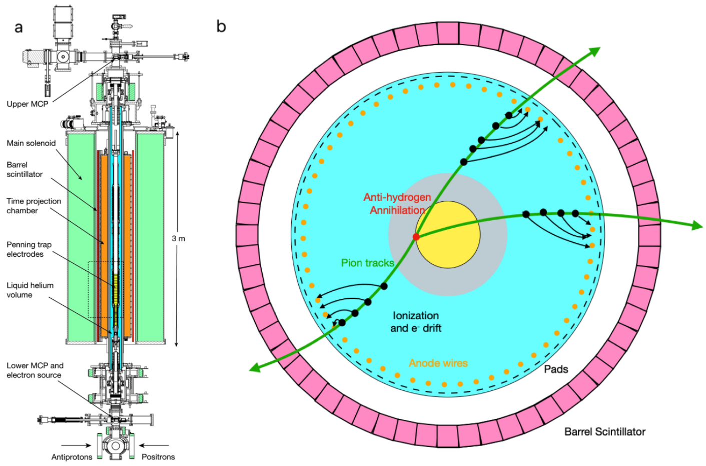

Figure 2. a. An overview of the ALPHA-g apparatus. Reproduced from [7]. CC BY 4.0. b. A diagram of an annihilation detected by the ALPHA-g TPC (blue) and the BSC (pink).

to a data acquisition rack. They are digitized by an analog-to-digital-converter (ADC) based on the GRIF-16 ADC [12], and a TRB3 time-to-digital-converter (TDC) [13].

The TRB3 TDC achieves a time resolution much shorter than a 5 ns clock cycle by passing an incoming signal through an FPGA delay chain. Each element has a characteristic delay time which must be determined using data. This "fine time" calibration is stable over a few years.

Beyond this calibration, the times from the TDC show variation of tens of nanoseconds, indicating further calibrations are required to achieve the sub-nanosecond time resolution needed for cosmic ray identification. The calibration constants are determined on a run-by-run basis using data from cosmic rays which is already taken regularly in between experiment cycles. This method proceeds in three parts, which are described here.

3.1 Top-bottom offsets

In experiments with multiple TDC channels, each channel will have a characteristic offset which must be subtracted, due to differing cable lengths and other factors. They are typically calibrated by injecting a simultaneous test pulse across all channels. In the BSC, these offsets were much larger than expected, due to internal offsets in the TRB3 TDC. Furthermore, these offsets change upon power cycling the TRB3 TDC; given the inclination of the TRB3 in our system to periodically crash, this necessitates a continuous calibration. Furthermore, problems with the test pulse circuit prevented implementing routine test pulse calibration runs.

The most important offset is between the top and bottom channels of a single bar, as this is needed to find the hit position. These are calibrated first using an independent method. Cosmic ray tracks from the TPC detector are matched to BSC hits, and an "expected" hit height is found by extrapolating the TPC track into the BSC volume. The measured hit height is determined using the time difference between the top and bottom SiPM signals. The offset between top and bottom is then obtained by comparing the expected and measured hit height, seen in figure 3a.

2025 JINST 20 C05007

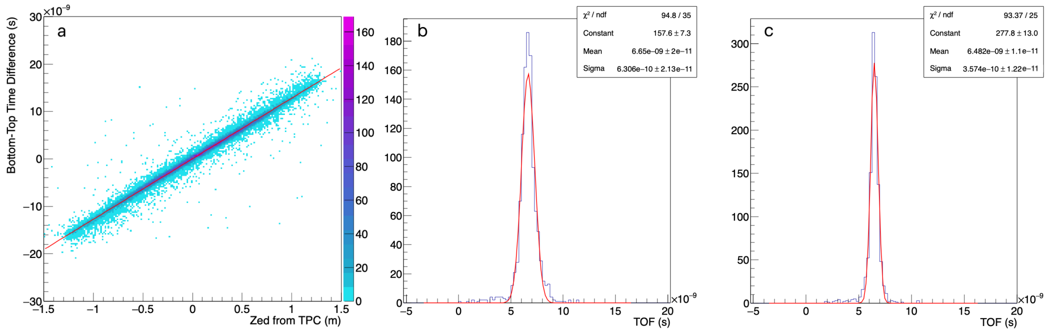

Figure 3. a. The bottom-top time difference for cosmic rays in a bar vs expected height from TPC. The linear fit is used to extract the top-bottom offset. b. Gaussian fit of time difference between two bars. c. The same data after applying an optimized time walk correction.

3.2 Bar-to-bar offsets

The next step is to obtain the characteristic offset of each bar. This is done by first extracting the time difference between each pair of bars, using the subset of cosmic ray events that hit exactly those two bars. The first bar is defined as the one with the higher hit position, taking advantage of the steep angle of incidence of cosmic rays. The time difference between the hit time (the average of top and bottom times) of each bar is plotted and fit with a Gaussian, seen in figure 3b. The mean of the Gaussian fit is recorded as the difference between the two bars.

The difference between two bars i, j with characteristic offsets t_i, t_j is given by $d_{i,j} = t_j - t_i$. Summing this equation over the subset G_i of bars j for which $d_{i,j}$ was fit successfully yields the following equation, which was solved iteratively to recover the characteristic offset of each bar t_i:

$$t_i = \frac{1}{|G_i|} \sum_{j \in G_i} d_{i,j} + \frac{1}{|G_i|} \sum_{j \in G_i} t_j \tag{3.1}$$

3.3 Time walk correction

Two pulses with the same shape cross a fixed threshold at a different time depending on their sizes; a larger amplitude pulse will cross the threshold sooner. This is known as the "time walk" effect. To correct for this in analysis, each SiPM waveform is digitized by an ADC as well as a TDC. The pulse height is extracted from the ADC waveform; in cases where the waveform is saturated, an empirical fit function is used to recover the true SiPM pulse height.

Traditionally, a large sample of data is used to determine the relationship between pulse height and TDC time. However, this approach requires events with a well-defined zero time, such as the bunch crossing time in a collider experiment, which is not available in ALPHA-g. Instead, a form $\delta t = k/\sqrt{A}$ was used for the time walk, which arises mathematically for a pulse with a quadratic rise. Here, A is the pulse height, and k is a calibration constant which was determined individually for each bar end. To determine k, the time difference between one bar and its opposite bar was plotted, as in section 3.2. Many values of k were tried, with the final value chosen to minimize the width/sigma of the Gaussian fit, as shown in figure 3c.

2025 JINST 20 C05007

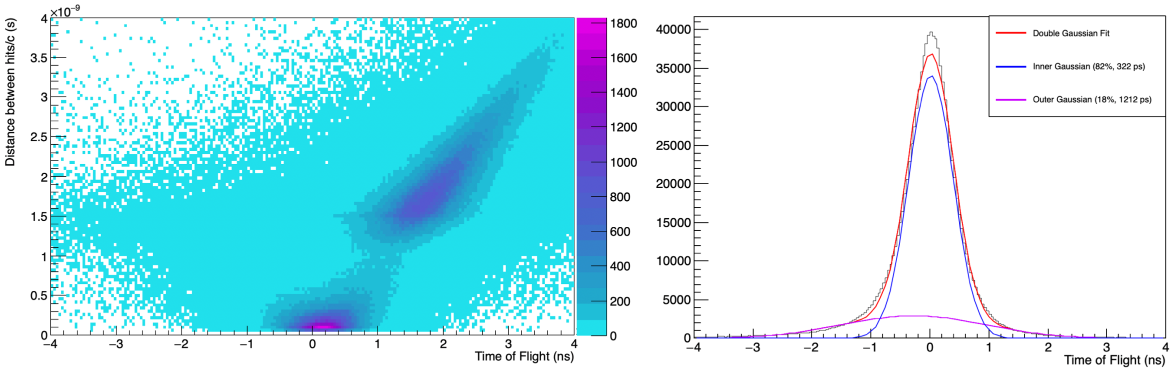

Figure 4. a. Measured time of flight of cosmic rays plotted against the physical distance between the two hits. Data along the diagonal indicates cosmic rays traveling at the speed of light. b. The residual time of flight corrected for physical distance, i.e. the diagonal projection of (a), fit with a double Gaussian function.

4 Results and outlook

Using this method, the time of a hit in the BSC is calculated as:

$$t = (t_{\text{top}} + \delta t_{\text{top}} + t_{\text{bot}} + \delta t_{\text{bot}})/2 + t_i \tag{4.1}$$

Here, $t_{\text{top/bot}}$ are the measured top/bottom hit times, $\delta t_{\text{top/bot}}$ are the time walk corrections for that bar, and t_i is the characteristic bar offset. Time of flight is calculated by subtracting two of these hit times. This yields a final time-of-flight resolution of 322 ps as shown in figure 4.

To reject the cosmic ray background, a boosted decision tree classifier was trained using ROOT's TMVA toolkit [14]. For the gravity paper, this included only spatial information from the TPC and BSC, and reduced the background rate from 70 Hz to 0.2 Hz. The inclusion of time of flight data, with the calibration presented here, has further improved this background rate to 0.014 Hz. This improved rejection is more than sufficient to remove the background from a 600 second measurement, as shown in figure 5. Such an improvement of the background rate will open new possibilities for ALPHA-g which necessitate releasing anti-atoms over a timescale of many minutes or hours, paving the way for future techniques and expanding the reach of the ALPHA-g physics program to further probe the gravitational behavior of antimatter.

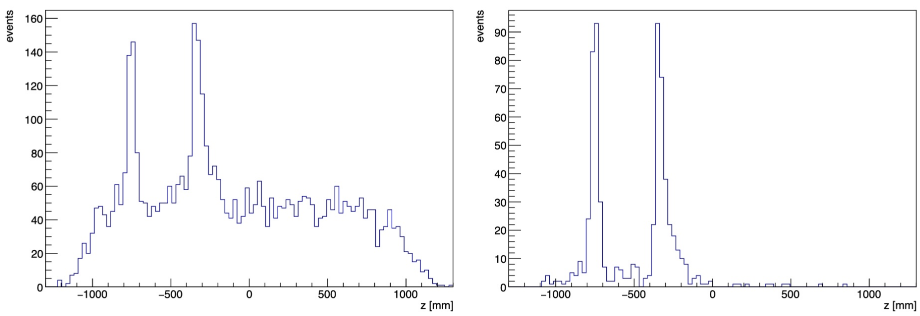

Figure 5. Annihilation positions of anti-hydrogen atoms collected over 2 hours, and released over 600 seconds. Shown without (left) and with (right) the time-of-flight based TMVA background rejection algorithm.

2025 JINST 20 C05007

References

[1] ALPHA collaboration, *Trapped antihydrogen*, *Nature* **468** (2010) 673.

[2] ALPHA collaboration, *Observation of the 1S-2S transition in trapped antihydrogen*, *Nature* **541** (2016) 506.

[3] ALPHA collaboration, *Observation of the hyperfine spectrum of antihydrogen*, *Nature* **548** (2017) 66.

[4] ALPHA collaboration, *Observation of the 1S-2P Lyman-α transition in antihydrogen*, *Nature* **561** (2018) 211.

[5] ALPHA collaboration, *Investigation of the fine structure of antihydrogen*, *Nature* **578** (2020) 375 [*Erratum ibid.* **594** (2021) E5].

[6] ALPHA collaboration, *Laser cooling of antihydrogen atoms*, *Nature* **592** (2021) 35.

[7] ALPHA collaboration, *Observation of the effect of gravity on the motion of antimatter*, *Nature* **621** (2023) 716.

[8] C. Carli et al., *ELENA: Bright Perspectives for Low Energy Antiproton Physics*, *Nucl. Phys. News* **32** (2022) 21.

[9] C.M. Surko, R.G. Greaves and M. Charlton, *Stored positrons for antihydrogen production*, *Hyperfine Interact.* **109** (1997) 181.

[10] Eljen Technology, *Plastic Scintillators EJ-200, EJ-204, EJ-208, EJ-212*, (2024), https://eljentechnology.com/products/plastic-scintillators/ej-200-ej-204-ej-208-ej-212, Accessed: 2025-02-13.

[11] ON Semiconductor, *MicroJ Series High-Performance Diodes*, (2024), https://www.onsemi.com/download/data-sheet/pdf/microj-series-d.pdf, Accessed: 2025-02-13.

[12] A.B. Garnsworthy et al., *The GRIFFIN data acquisition system*, *Nucl. Instrum. Meth. A* **853** (2017) 85 [arXiv:1711.06236].

[13] A. Neiser et al., *TRB3: a 264 channel high precision TDC platform and its applications*, 2013 *JINST* **8** C12043.

[14] TMVA collaboration, *TMVA — Toolkit for Multivariate Data Analysis*, physics/0703039.

2025 JINST 20 C05007